Apatite Application to Investigate Magmatic Evolution of Zouzan Granites, NE Lut Block

S.A. Mazhari[1*], R. Sharifiyan Attar[1]

1. Department of Geology, Payame Noor University, 19395-4697 Tehran, Iran.
Received 27 November 2011; accepted 20 April 2012

Abstract

Apatite minerals of I-type Zouzan granitoids and typical garnet-bearing S-type granites have been analyzed by electron microprobe to define trace element concentrations and compare them in different granites. Zouzan granites are composed of apatites with lower Fe, Mn, Na and HREE and higher REE and ∑REE relative to S-type ones. Trace elements abundances of apatite often vary with some parameters of the host rock, especially aluminum saturation index (ASI). Strontium content of apatite is very sensitive to whole-rock composition and binary diagrams of SrO- trace elements could be used to discriminate different granites and realize magmatic evolution in a single phase. The apatite concentration of Fe, Mn, Na and HREE increases during magmatic fractionation in Zouzan pluton, while Sr and REE decreases. The difference of REE concentrations in apatites of mafic and felsic rocks of Zouzan granitoids relates to the coeval or earlier crystallization of amphibole and titanite, respectively. Acicular apatites which are present in granodiorites and mafic microgranular enclaves show exceptionally dissimilar composition in comparison with other apatites in the same sample and host rock geochemistry. Extraordinary high levels of Fe, Mn, LREE, $(Sr_{apatite}/Sr_{bulk-rock})>1$ and unusual low HREE indicate that a more mafic magma was involved in magma genesis of Zouzan pluton and confirms magma mixing.

Keywords: Apatite, Granite, I-type, S-type, Trace elements, Zouzan pluton.

1. Introduction

Apatite appears as a ubiquitous accessory mineral in different igneous, metamorphic and sedimentary rocks because it is stable in various geological processes. Apatite could be occurred at room temperature and 1 atm pressure from aqueous solutions, and is also stable at least in upper mantle conditions up to 2.5 GPa and 1350˚C [1]. Apatite is an early crystallizing and long-lasting phase that reaches saturation during the evolution of a range of silicate melts [2]. Ideal formula of apatite is $Ca_{10}(PO_4)_6(F, OH, Cl)_2$, but it is also an excellent host of some trace elements such as REE, Sr, U, and Th in the natural system which are useful not only for understanding ore genesis [3], but also in the field of mineral exploration [4]. These characteristics make petrologist analyze apatite minerals in different rocks. Meurer and Natland used apatite chemistry to reveal magmatic evolution of oceanic cumulates [5]. Boyce and Hervig utilized apatite to monitor late-stage magmatic processes in volcanic activities [6]; and apatite potential for petrogenesis of different ultramafic, alkaline and carbonatite rocks have been studied by Brassini et al.[7] and Ronsbo [8]. In this regard, granites could attract the most attention of apatite studies between various rocks.
Sha and Chappell found that apatites can concentrate many minor and trace elements whose abundances and

----
*Corresponding author.
E-mail address (es): ali54894@yahoo.com*

ratios are sensitive to factors controlling the fundamental differences between I- and S-type granites and suggested that the results have important implications for identifying different types of granites and potential significance for determining the provenance of sedimentary rocks [9]. Afterwards, the application of apatite has been growing to clarify magmatic processes (e.g. [10], [11], [12]).

Geochemical composition of apatites could be detected by modern analytical instruments, so that major oxide components in separated grains have been defined by electron micro probe analyzes (EPMA) and minor and trace elements analyzed by laser ablation inductivity coupled mass spectrometry (LA-ICP-MS) techniques (e.g. [4], [9], [12]). Since the concentration of many trace elements is more than detection limit of EPMA, some authors used EPMA for chemical determination of apatite trace elements, too (e.g. [10]). In this study, we select granitic samples of Zouzan pluton to detect major and trace element concentration of apatites in thin polish sections by EPMA and define accessory minerals by SEM. Petrographical and whole-rock geochemical characteristics of this pluton have been previously studied [13]; and our new data shows that apatite composition in association with careful investigation of accessory mineral relations in granitic samples are key factors to distinguish detail petrogenesis history of these rocks.

2. Geological Setting and Petrological Implications of Zouzan Pluton

The study area is situated 120 km northeast of Birjand, in the NE of Lut block, Eastern Iran (Fig. 1a). The Lut block extends over 900 km in a NS direction and 200 km wide in EW direction [14]. Its boundary is confined by Doruneh fault in the north, Juz-Morian basin in south, Nayband fault and Shotori range in the west, and East Iranian range and Nehbandan fault in the east. The Lut block is part of the central east Iranian microcontinent, including the Tabas, Yazd, and Posht-Badam blocks [15]. The Iranian plate was fragmented after collision with Turan plate and the central east Iranian microcontinent represents one of those fragments [16].

The paleotectonic setting of Lut block is controversial and various scenarios have been defined by different authors. The Lut region reveals a platform character in its sedimentation during the Paleozoic. Intensive orogenic movements during Mesozoic and Tertiary led to breaking and splitting of this platform, which resulted in a reactivation of different lineament and finally Central Iran separated into mosaic-like blocks [17]. NS Shotori range stands between the Central Lut and Tabas block. The Lut Block underwent an anti-clockwise rotation of 30–90° relative to Eurasia due to the collision of India (and Afghanistan) with Eurasia during Tertiary [18]. Tirrul et al. supposed existence of an oceanic plate between the Lut block and the Afghan block which subducted under the Lut block in the Tertiary [19]. Although the geochemical data from the Lut block are insufficient to design its geotectonic environment, data from volcanic rocks from different parts of the Lut block point to calc-alkaline magmatism in a convergent tectonic environment ([20], [21]).

The Zouzan pluton has nearly circular exposure with 8-12 km wide and 14 km long (Fig.1b). The main lithological units in this area are Eocene volcanic-volcanoclastics and Paleocene sedimentary rocks, which are intruded by Zouzan pluton (Fig.1b). There is not any radiometric data about this pluton, but on the basis of field relation, they are ascribed to Oligocene [22]. There are contact metamorphic rocks with several hundred thicknesses in some locations (Fig.1b). The Zouzan pluton has bimodal nature and consists of the major occurrence of felsic and minor mafic rocks (Fig.2). It is not possible to separate mafic rocks as a distinct unit in map; so the location of mafic samples is shown within felsic unit in Fig.1b.Mafic rocks appear as small stock or dyke units in granitoids; and the contact between them are sharp in the most outcrops (Fig.2). Geochemical characteristics suggest mafic rocks are genetically unrelated to granitoids and were derived from partial melting of metabasalt sources in a subduction setting [13]. So, mafic rocks won't be considered in this article.

Granitoids are massive with no signs of magmatic foliation, however, structural deformation is abundant. Also, aplitic and evolved granitic veins and pegmatoid dikes cross-cut some outcrops; and quartz or aplitic veinlets fill the joints and fractures. Mafic microgranular enclaves (MME) are profound in granitoids (Fig.3). They are unevenly distributed in Zouzan granitoids, but their abundance in more mafic parts (granodiorites) is higher than those occur in felsic ones (granites). Physical and petrographical textures in MME imply magma mingling role in the petrogenesis of Zouzan pluton [13].
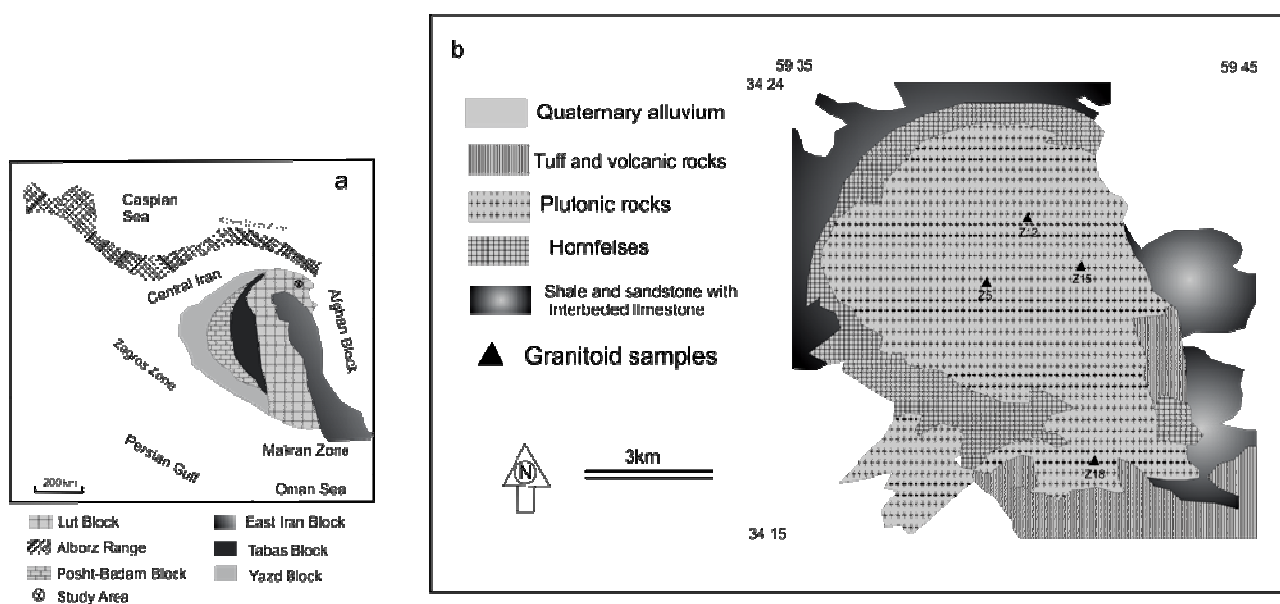
Fig1. (a) Map showing the position of the Lut block in Iran relative to the adjacent blocks (modified after [20]). (b) Simplified geological map of studied area (modified after Blourian and Safari, [22]).
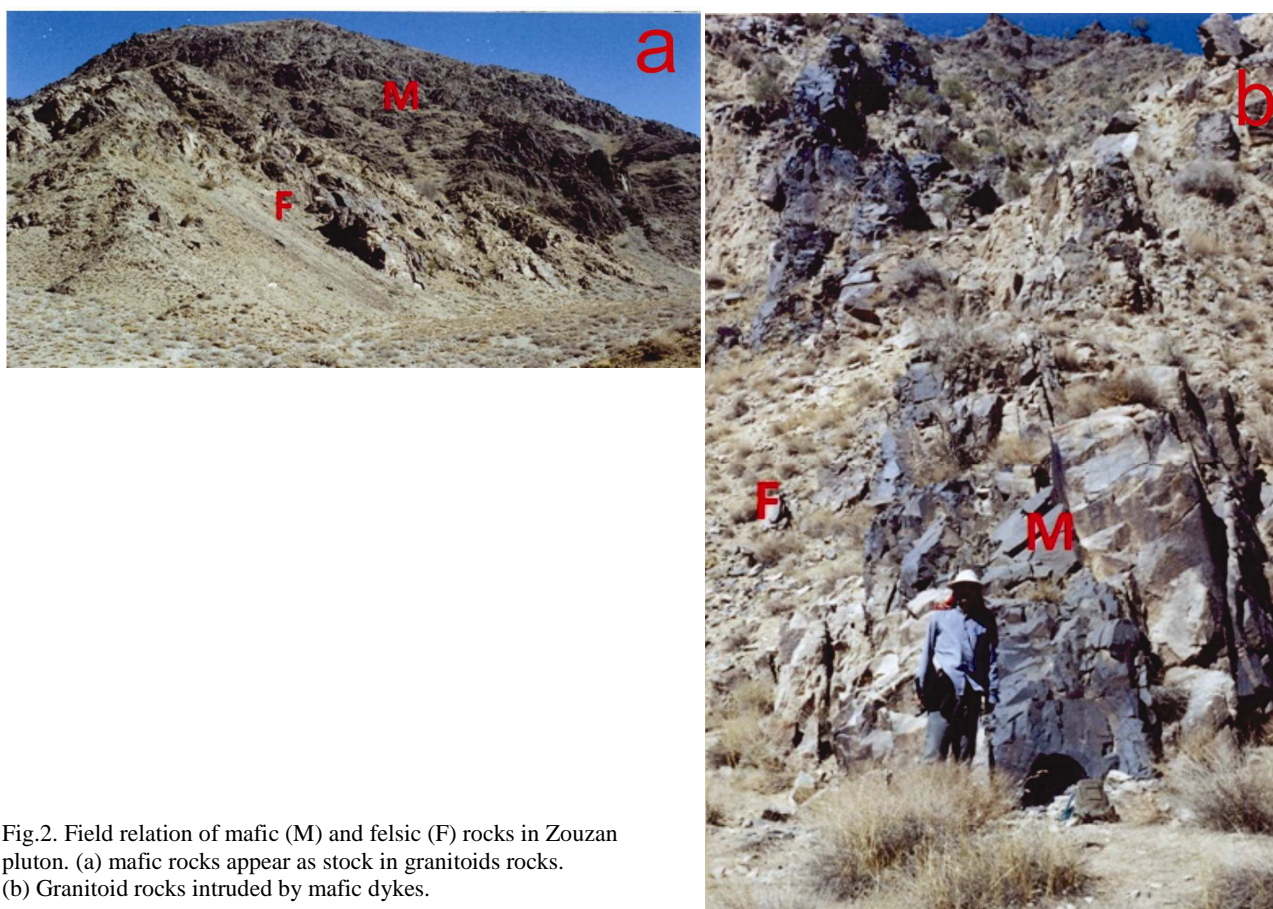
Fig.2. Field relation of mafic (M) and felsic (F) rocks in Zouzan pluton. (a) mafic rocks appear as stock in granitoids rocks. (b) Granitoid rocks intruded by mafic dykes.

Fig.3. Different mafic microgranular enclaves (MMEs) in Zouzan granitoids. Rounded (a), elongated (b) and irregular (c) mafic microgranular enclaves with sharp contact to host granitoids. (d) coarser grained enclave with porphyritic minerals (black arrow) in junction to fine-grained MME (yellow arrow).

3. Sample Selection and Analytical Procedure

As mentioned above, comprehensive data about whole rock geochemistry of Zouzan pluton have been discussed in [13]. For this research, four samples of granitoids were elected to cover complete chemical range of felsic rocks in Zouzan pluton. Furthermore, two samples of well-known peraluminous S-type granites of Iran were analyzed to compare their composition with Zouzan sample. These two samples are composed of Baneh and Shirkuh garnet- bearing granites. Previous studies approved that they are typical S-type granites generated by partial melting of crustal rocks ([23], [24]).

Major elements and Zr were analysed by XRF in the laboratory of Geological Survey of Iran and trace element concentrations were analyzed by ICP-MS facility at ACME laboratory, Vancouver, British Columbia. In XRF analyses, typical precision was better than ±1.5% for an analyte concentration of 10 wt%, and ±2.5% for 100 ppm Zr. All samples for ICP analysis were dissolved using an alkali fusion (LiBO2/LiB4O7) method. Reproducibility, based on repeat analyses, for most trace elements has an uncertainty of ±5.0% if the concentrations are >100 ppm and ±10% for those with <100 ppm.

Accessory mineral relations and apatite geochemistry were defined by SEM and JEOL JXA-8900R electron microprobe analyses at the Department of Earth Science, Academia Sinica of Taiwan. Operating conditions were 15 kV, 25 nA beam current and a beam diameter of 1–5 μm, depending on the apatite grain size. Care was taken in the determination of F and a PC1 (multi-layer crystal) was used to eliminate the potential interference from the P 3rd-order line.

4. Petrography

Detail petrography and textural relations of Zouzan pluton is reviewed by [13]. Modal composition of granitoids in Zouzan pluton plots in the granodiorites to granite fields. They have a subhedral granular texture and contain quartz (8-20%), plagioclase (20-50%), K-feldspar (3-15%), amphibole (2-23%), biotite (2-17%), zircon, apatite, titanite and Fe-Ti oxides. Chlorite, sericite, epidote and secondary titanite are secondary minerals observed in some samples. Selected samples for this study include two samples of granodiorites (Z5 and 12) and two granites (Z15 and Z18) which were analyzed by SEM and EPMA for more investigation in apatite geochemistry and accessory mineral composition of Zouzan granitoids. Major and accessory mineral associations of these samples are presented in Table1. SEM study shows that most of Fe-Ti oxides are magnetite and ilmeno-magnetite which partially replaced by secondary hematite.

Zircon, apatite, allanite and titanite are ubiquitous in all samples, although, titanite abundance in granodiorites is more than granite samples. There is minor xenotime in granodiorite samples, while it is absent in granites. Minor pyrite grains are present in Z5, Z15 and Z18 samples and scarce sphalerite could be observed in Z12 (Table1). SEM data reveals that Zouzan granitoids includes magnetite, allanite and titanite as accessory minerals which are typical for I-type granites ([25], [26]). This is in congruent with whole rock geochemical data which suggest Zouzan granitoids have been formed by partial melting of mantle-derived mafic rocks [13]. Apatite occurs as various forms in granitoid samples (Fig.4). Circular and elongated needle grains of apatite are the normal form in all samples (Fig.4 a,b,d) but acicular apatites appear only in MME and granodiorite samples (Fig.4 d). Normally, apatite becomes available as inclusion in major minerals (feldspar, quartz, amphibole and biotite); but in granodiorite samples it also appears as inclusion in euhedral titanite grains.

Two samples of typical S-type granites of Baneh and Shirkuh plutons were studied to compare their accessory minerals by Zouzan granitoids. Zircon and apatite are also common accessory minerals in these samples, but titanite and allanite are absent. Ilmenite is the most plentiful Fe-Ti oxide and xenotime is more abundant than Zouzan samples. Another distinguish accessory mineral in S-type granites is monazite and the concentration of sulfide minerals are higher than Zouzan granitoids..

Table 1. Modal composition (V%) and accessory minerals of studied samples. Qtz= quartz; Kfd= K-feldspar; Plg= plagioclase; Amph= amphibole; Bio= biotite.

Sample ID	Qtz	Kfd	Plg	Amph	Bio	Accessory minerals
Z5	14	13	37	28	8	Apatite+zircon+titanite (abundant) + allanite+ sphalerite+ xenotime
Z12	19	14	36	21	10	Apatite+zircon+titanite (abundant) + allanite+ pyrite+ xenotime
Z15	25	30	26	2	17	Apatite+zircon+titanite (rare) + allanite+ pyrite
Z18	23	35	25	2	15	Apatite+zircon+titanite (rare) + allanite+ pyrite

5. Results

In this study four samples were selected to represent complete chemical range of granitoid rocks. Major and trace element composition of these samples are presented in Table2 in addition to two S-type samples of Baneh and Shirkuh plutons. As previously discussed, geochemical data of Zouzan, Baneh and Shirkuh plutonic rocks have been reviewed by [13], [23] and [24]. Felsic rocks of Zouzan are metaluminous to slightly peraluminous I-type granitoids and exhibit high-K calc-alkaline characteristics. Major and trace element compositions suggest mafic sources for the formation of Zouzan granitoids. Partial melting of subducted mantle wedge in association of fractionation and interaction with mafic magma has led to the formation of different granitoid rocks in the Zouzan pluton [13].

Over 80 analyses for major and trace oxides have been carried on apatite grains of studied samples. The results of 20 representative apatites are presented in Table3. Furthermore, two columns of this table show mean values of six and four analyzed apatite of Baneh and Shirkuh S-type granites, respectively.

The major constituents of of apatite, CaO and P_2O_5, both show limit variation; the most common values are from 52.8 to 54.5 wt.% CaO and from 40.6 to 41.8 wt.% P_2O_5. SiO_2 generally varies between 0.1-0.3 wt% and doesn't show any regular correlation with the host rock variation or other elements of apatite (Table3).

MnO and FeO vary between 0.07-0.35 and 0.01-0.21 wt%, respectively. These values are completely lower than typical S-type granites which include higher contents of these elements (Table3). These oxides exhibit different behavior during various apatites, so that their concentration increases from more mafic granodiorite (Z5) to more felsic granite (Z15). Several authors insisted on the role of aluminum saturation index of host magma [ASI, calculated as molecular Al2O3/(Na2O + K2O + CaO)] in distribution of minor and trace elements of apatite mineral (e.g. [9]. [12]). Zouzan apatites show similar trend and iron and manganese concentration increase with ASI (Fig.5 a,b). Acicular apatites which are common in granodiorites and MME depict distinct chemical composition which is obvious in Table3 and Fig.5. They have higher FeO and MnO relative to other apatites in the same sample (Fig.5 a,b).

Studied apatites are fluorapatites, which is typical of igneous apatite (1.9–3.2 wt.% F), where the F content is known to increase with differentiation [27]. More felsic rocks of Zouzan granite with higher ASI exhibit relatively more F in their apatite (Fig. 5C).

Na_2O generally varies from 0.04 to 0.17 wt% in Zouzan granitoids. They show regular correlation between ASI and Na_2O content, so that sodium concentration increases in peraluminous granites (Table3 and Fig. 5d). S-type granites have higher Na_2O; and acicular apatites are enriched relative to other apatites in the same sample (Fig. 5d).

SO_3 concentration differs from 0.01-0.07 wt% without any systematic variation (Table3). It is not concordant with Australian granites which SO_3 falls with increasing ASI of the host rocks [9]. The SO_3 content of apatite depends on oxygen fugacity (e.g. [4], [2]). Mineral accessory composition, especially Fe-Ti oxides, suggests similar oxidizing environment during the formation of different rocks from Zouzan granitic magma; therefore, SO_3 shows irregular variation in granitoids.

SrO varies widely in apatites of different granitoids (0.06-0.68 wt%). Apatite strontium doesn't demonstrate meaningful relation with ASI, but is consistent with Sr concentration of whole rock (Fig. 6a). Because Sr^{2+} and Ca^{+2} have very similar ionic radii and other chemical properties, Sr contents in apatites should mimic those in the host rocks [4]. In this regard, acicular apatites show abnormal high concentration of Sr which will be discussed in the next section.

ThO_2 and UO_2 show limit range and irregular correlation with the host rock composition (0.03-0.05 and 0.01-0.04 wt% for ThO_2 and UO_2, respectively). Acicular apatites, again, mark uncommon concentrations of Th and U. Thorium and uranium concentration of these apatites are below the detection limit of EPMA in contrast to other apatites in I-type granites (Table3). In other side, Th and U concentration in Baneh and Shirkuh granites is very low similar to other S-type granite (e.g. [9], [12]).

Apatite contains significant amounts of rare earth elements (REE) substituting for Ca ([8], [27]). This substitution has been shown previously to be coupled with substitution of Na^+ for Ca^{2+} and Si^{4+} for P^{5+} to achieve charge balance [9]. Our data approved that the concentration of most REE oxides are more than detection limit of EPMA (Table3). The total REE concentration normally ranges between 0.21-0.45 wt% in Zouzan granitoid apatites; but acicular apatites in granodiorite samples have exceptionally high REE (>0.70 wt%). REE concentrations in garnet-bearing granites are low alike typical S-type granites [9]. Internal distribution between REEs is different among various apatites. As it is clear from Table 2 and Figures 2 and 3, LREE (La_2O_3+ Ce_2O_3+ Pr_2O_3+ Nd_2O_3) and HREE (Dy_2O_3+ Er_2O_3+ Yb_2O_3) concentration differ considerably from more mafic granodiorites to felsic granites (Table 3). Granodiorite samples are enriched in LREE and depleted in HREE relative to granitic samples (Fig. 5 e,f). These data shows REE content and its distribution in apatite is dependent on the whole rock chemistry, so that LREE decrease from >0.40 to 0.2 when ASI increases from 0.9 to 1.06.

Table 2. Major (wt% oxides) and trace element composition (ppm) of studied samples. B= Baneh and Sh= Shirkuh S-type garnet-bearing granites.

Sample ID	Zn12	Zn5	Zn18	Zn15	Sh	B
Rock type	granodiorite	granodiorite	granite	granite	Grt Granite	Grt Granite
SiO_2	66.916	64.993	68.523	72.285	69.77	70.86
TiO_2	0.719	0.823	0.559	0.238	0.39	0.14
Al_2O_3	14.171	14.409	14.729	13.852	14.73	15.11
FeOt	4.543	4.904	3.721	1.856	3.84	3.12
MgO	1.627	2.205	1.667	0.867	1.01	0.94
MnO	0.067	0.064	0.046	0.044	0.07	0.12
CaO	2.493	3.41	2.493	1.502	2.17	0.48
Na_2O	3.967	3.836	3.43	3.399	2.58	3.12
K_2O	3.92	3.192	3.989	4.335	4.53	5.52
P_2O_5	0.196	0.237	0.151	0.095	0.16	0.16
L.OI.	1.12	1.83	0.81	1.09	1.01	0.6
Total	99.74	99.90	100.12	99.56	100.26	100.17
Rb	157	112.2	155.4	189	156.6	167.7
Cs	0.2	4.4	0.3	1.1	6.63	
Sr	363.5	401.5	295.8	181.3	128.3	232.4
Ba	606.9	610	523.3	581	442.4	501.5
Y	22.4	16.4	20.5	30.7	27.7	26.8
Nb	13.2	12.3	12.6	25.4	12.5	9.7
Ta	0.7	0.7	1.3	2.7	1.46	0.66
Zr	367.5	324.9	253	190	119	242
Th	22	12	18	21	32.2	21.6
La	26.9	26.82	32.53	37.18	41.19	6.88
Ce	59.04	53.33	64.09	76.07	60.14	14.64
Pr	7.03	5.76	6.66	7.54	6.95	1.13
Nd	25.01	20.93	24.22	25.89	25.53	3.52
Sm	4.61	4.07	4.21	4.25	5.82	1.39
Eu	0.91	1	0.9	0.89	1.14	0.17
Gd	4.18	3.94	3.65	3.97	6.29	1.54
Tb	0.77	0.72	0.67	0.7	0.9	0.35
Dy	3.97	3.95	3.55	3.39	5.28	3.92
Ho	0.74	0.73	0.65	0.71	1.01	0.18
Er	2.27	2.19	2.02	2.03	2.91	2.37
Tm	0.35	0.34	0.32	0.34	0.15	0.75
Yb	2.39	2.23	2.19	2.27	2.49	1.28
Lu	0.38	0.35	0.33	0.35	0.31	0.17

6. Discussion

Trace element data for apatite from different granitic rocks confirms that the concentration of these elements could be detected by EPMA (Table3). These elements show broad ranges in concentration and relative abundances and exhibit regular variation according to specific parameters. Trace element abundances of apatite often vary with some parameters of the host rock, such as the oxidation state, SiO2 content, total alkali and ASI values [4]. EPMA data from apatites of Zouzan granitoids suggest that the variation in trace-element concentrations in apatites is strongly related to whole rock ASI (Fig.5). Furthermore, trace element content of apatite is dependent on the genesis and environmental condition of magma generation. Trace elements arrays in Fig.5 approve different apatite compositions of S and I- type granites. These differences could apply to distinguish different granites (e.g. [9], [12]).

Apatites of Zouzan granites contain more Fe and Mn than typical S-type granites of Iran. Anymore, FeO and MnO in apatite increase during magmatic evolution of Zouzan granitoids and maximum values reach in more evolved granitic samples (Fig.5 a,b). Petrological studies confirm crystal fractionation in Zouzan granitoids [13], so iron and manganese concentration which increase in more evolved rocks and felsic granitoids would concentrate higher Fe and Mn in their apatites.

Table 3. Representative microprobe analyses (in wt.% oxide) of apatite from the Zouzan Granitoids. Two last columns are mean values of Baneh (n=6) and Shirkuh (n=4) apatites.

Sample ID	Zn12-1	Zn12-2	Zn12-3	Zn12-4	Zn12-5	Z12-6(ac)	Z12-7(ac)	Z5-1	Z5-2	Z5-3	Z5-4
SiO_2	0.22	0.18	0.15	0.17	0.13	0.25	0.31	0.17	0.24	0.23	0.16
FeO	0.06	0.08	0.05	0.01	0.06	0.15	0.16	0.03	0.02	0.03	0.01
MnO	0.15	0.33	0.12	0.07	0.23	0.14	0.12	0.25	0.11	0.13	0.12
CaO	54.05	54.41	54.28	54.51	54.17	52.85	53.75	54.27	54.36	54.38	54.41
Na_2O	0.04	0.08	0.05	0.11	0.09	0.08	0.07	0.05	0.07	0.05	0.08
P_2O_5	41.73	40.98	41.77	41.69	41.85	41.35	40.89	41.33	41.33	40.88	41.47
F	2.26	2.37	2.45	2.12	2.51	2.96	2.87	2.22	1.96	2.13	2.04
Cl	1.12	1.15	0.85	0.71	0.34	0.85	0.61	0.91	1.31	1.26	0.94
SO_3	0.05	0.06	0.05	0.04	0.07	0.01	b.d.	0.04	0.05	0.05	0.04
SrO	0.12	0.21	0.15	0.14	0.19	0.67	0.59	0.23	0.29	0.25	0.26
ThO_2	0.05	0.04	0.05	0.04	0.03	b.d.	b.d.	0.05	0.03	0.06	0.05
UO_2	0.01	0.03	0.01	n.d	0.04	0.03	0.01	0.02	0.03	0.01	0.01
La_2O_3	0.06	0.05	0.05	0.06	0.05	0.09	0.1	0.06	0.07	0.05	0.06
Ce_2O_3	0.17	0.22	0.15	0.28	0.21	0.46	0.39	0.23	0.15	0.31	0.25
Pr_2O_3	0.04	0.02	0.03	0.03	0.04	0.08	0.09	0.02	0.02	0.03	0.04
Nd_2O_3	0.06	0.08	0.06	0.05	0.08	0.21	0.16	0.05	0.08	0.06	0.06
Sm_2O_3	0.02	0.03	0.01	0.01	0.02	0.02	0.04	0.03	0.01	0.01	0.02
Gd_2O_3	0.02	0.02	0.02	0.01	0.02	0.01	0.02	0.01	0.01	0.03	0.01
Dy_2O_3	0.01	b.d.	0.01	0.01	0.01	b.d.	0.02	b.d.	0.01	0.01	0.01
Er_2O_3	b.d.	0.01	b.d.	b.d.	0.01	b.d.	b.d.	0.01	b.d.	b.d.	b.d.
Yb_2O_3	b.d.	b.d.	b.d.	b.d.	b.d.	b.d.	b.d.	b.d.	b.d.	b.d.	b.d.

Table 3. Continued

Sample ID	Z5-5 (ac)	Z5-6(ac)	Z18-1	Z18-2	Z18-3	Z18-4	Z15-1	Z15-2	Z15-3	B	Sh
SiO_2	0.21	0.19	0.19	0.21	0.18	0.14	0.23	0.15	0.19	0.022	0.05
FeO	0.21	0.19	0.05	0.08	0.1	0.08	0.14	0.12	0.16	0.22	0.23
MnO	0.17	0.11	0.25	0.31	0.22	0.28	0.31	0.28	0.35	0.41	0.53
CaO	53.14	53.06	54.29	53.96	54.37	53.58	54.31	53.98	54.13	54.07	54.02
Na_2O	0.05	0.07	0.07	0.12	0.09	0.11	0.13	0.17	0.15	0.28	0.44
P_2O_5	41.21	41.62	40.68	41.04	41.38	41.86	40.88	41.19	40.85	41.4	40.88
F	3.02	2.85	3.31	3.02	2.68	2.39	3.12	3.08	3.23	3	3.21
Cl	0.53	0.59	0.83	0.62	0.59	0.88	0.52	0.69	0.49	0.31	0.36
SO_3	0.02	0.01	0.03	0.07	0.04	0.03	0.03	0.04	0.06	b.d.	b.d.
SrO	0.68	0.65	0.09	0.12	0.08	0.11	0.06	0.08	0.09	0.01	0.13
ThO_2	b.d.	b.d.	0.04	0.05	0.04	0.05	0.05	0.03	0.05	b.d.	b.d.
UO_2	0.01	b.d.	0.01	0.03	0.01	0.02	0.02	0.02	0.01	0.02	0.02
La_2O_3	0.11	0.09	0.04	0.03	0.04	0.04	0.03	0.02	0.02	0.02	0.02
Ce_2O_3	0.37	0.41	0.11	0.17	0.15	0.13	0.09	0.1	0.06	0.02	0.03
Pr_2O_3	0.06	0.08	0.02	0.03	0.02	0.03	0.02	0.02	0.01	0.01	0.01
Nd_2O_3	0.14	0.15	0.05	0.04	0.04	0.03	0.03	0.03	0.04	0.01	0.02
Sm_2O_3	0.01	0.02	0.02	0.02	0.01	0.02	0.01	0.02	0.01	0.01	0.02
Gd_2O_3	0.02	0.01	0.01	0.02	0.02	0.01	0.01	0.01	0.02	0.02	0.02
Dy_2O_3	b.d.	b.d.	0.01	0.02	0.01	0.01	0.02	0.02	0.01	0.03	0.04
Er_2O_3	b.d.	b.d.	0.01	0.02	0.01	0.01	0.02	0.02	0.02	0.03	0.03
Yb_2O_3	b.d.	b.d.	b.d.	0.01	0.01	0.01	0.01	0.02	0.02	0.02	0.02

Na_2O apatite content of S-type granites is very higher than Zouzan granitoids (Table3 and Fig.5d). This difference could not be related to the whole-rock Na contents of either the granites or their source rocks. S-type granites contain the same or less Na than Zouzan granitoids (Table 3). Sha and Chappell

ascribed this difference to cation substitution mechanisms in apatite so that the replacement of Ca by Na is controlled by charge-balancing mechanisms [9]. Such interpretation could be considered for Na content diversity of apatites from Zouzan and S-type granites. Na_2O variation of apatites in different rocks of Zouzan granitoids confirms whole rock role in the sodium

concentration, at least in a magmatic phase because more felsic granites with higher ASI and Na_2O have higher Na_2O in their apatites (Fig.5).

Strontium plays as a unique element between trace element constituents of studied apatites. As previously referred, SrO variation in apatites is related to Sr content of host rock (Fig. 6a). By more investigation on Sr data, it is clear that there is good correlation between Sr and other trace elements of apatites (Fig.6a). Since apatite SrO content falls during magmatic differentiation of Zouzan granitoids, more evolved rocks include apatites with lower Sr and SrO is negatively correlated with FeO (Fig. 6b), MnO (Fig. 6c), F (Fig. 6d) and Na_2O (Fig. 6e). These diagrams indicate that Sr content of apatite could be use as an important factor to clarify magmatic revolution in granitic magmas and to discriminate different host-rocks.

Rare earth elements have notable concentration in the apatite structure and therefore, are potentially useful in petrological investigations. Zouzan apatites contain more ∑REE than S-type granites in accordance with I-type geochemical characteristics of whole rock [13]. Higher LREE and lower HREE are the other distinct features of Zouzan apatite relative to S-type granites (Figs 5 and 6). REE distribution in magmatic systems usually controls by accessory minerals (e.g. [28]). Among the common REE-retaining accessory minerals, apatite is high in all REE, zircon and xenotime are enriched in HREE, and monazite and allanite are characteristically enriched in LREE [28]. SEM data shows that S-type samples include considerable monazite while Zouzan granitoid lacks it (Table 1). So, the depletion of REE in S-type apatites can be attributed to the crystallization of monazite, before and/or concurrently with apatite, as monazite is one of the main accessory phases in these samples. In other side, apatites of Zouzan granitoids show intense depletion of HREE relative to S-type ones (Figs 5f and 6f; Table 3). This depletion should be related to relatively more HREE-rich accessory minerals competing for the HREE in the evolved melts when apatite crystallized. Amphibole is another mineral capable to concentrate HREE in addition to xenotime and zircon [28]. Zircon abundance is the same in all studied samples. Xenotime is more common in S-type samples, but Zouzan granites have plentiful amphibole which causes more depletion of HREE in coeval crystallized apatites. Among the Zouzan granitoids, granodiorite samples are more LREE enriched than granitic samples (Figs 5,6 e,f). The crystallization of LREE-rich minerals such as titanite before or together with apatite can significantly reduce the LREE enrichment of apatite (e.g. [12]).

SEM investigation show that apatite in granodiorite samples crystallized before titanite (the occurrence of apatite as inclusion in titanite), so apatites of these samples contain high LREE; in contrast to felsic

granitic samples which crystallized after some crystal fractionation processes include titanite as suggested by [13].

Acicular apatites in granodiorites and their mafic microgranular enclaves (MMEs) show completely different trace elements concentrations inconsistent with other apatite in the same sample and even inconsistent with host rock chemistry (Table 3 and Figs 5 and 6). They have extraordinary high Fe, Mn, Sr and LREE and low HREE concentration relative to other apatites. These unusual characteristics in apatite chemistry of granitic samples have been ascribed to the role of additional magmatic source(s) with different whole rock composition (e.g. [6]). Normally granite apatites have $(Sr_{apatite}/Sr_{bulk-rock}) < 1$ [9]; but this ratio in acicular apatites of Zouzan granodiorites is more. This high value of $(Sr_{apatite}/Sr_{bulk-rock})$ in apatite has been suggested as an indicator that a more mafic magma was involved in magma genesis [12]. Geochemical data and field relations in Zouzan pluton improved magma mixing processes during the formation of these rocks [13]; so acicular apatites of granodiorite samples and MMEs could be evidence of magma mixing in Zouzan pluton petrogenesis.
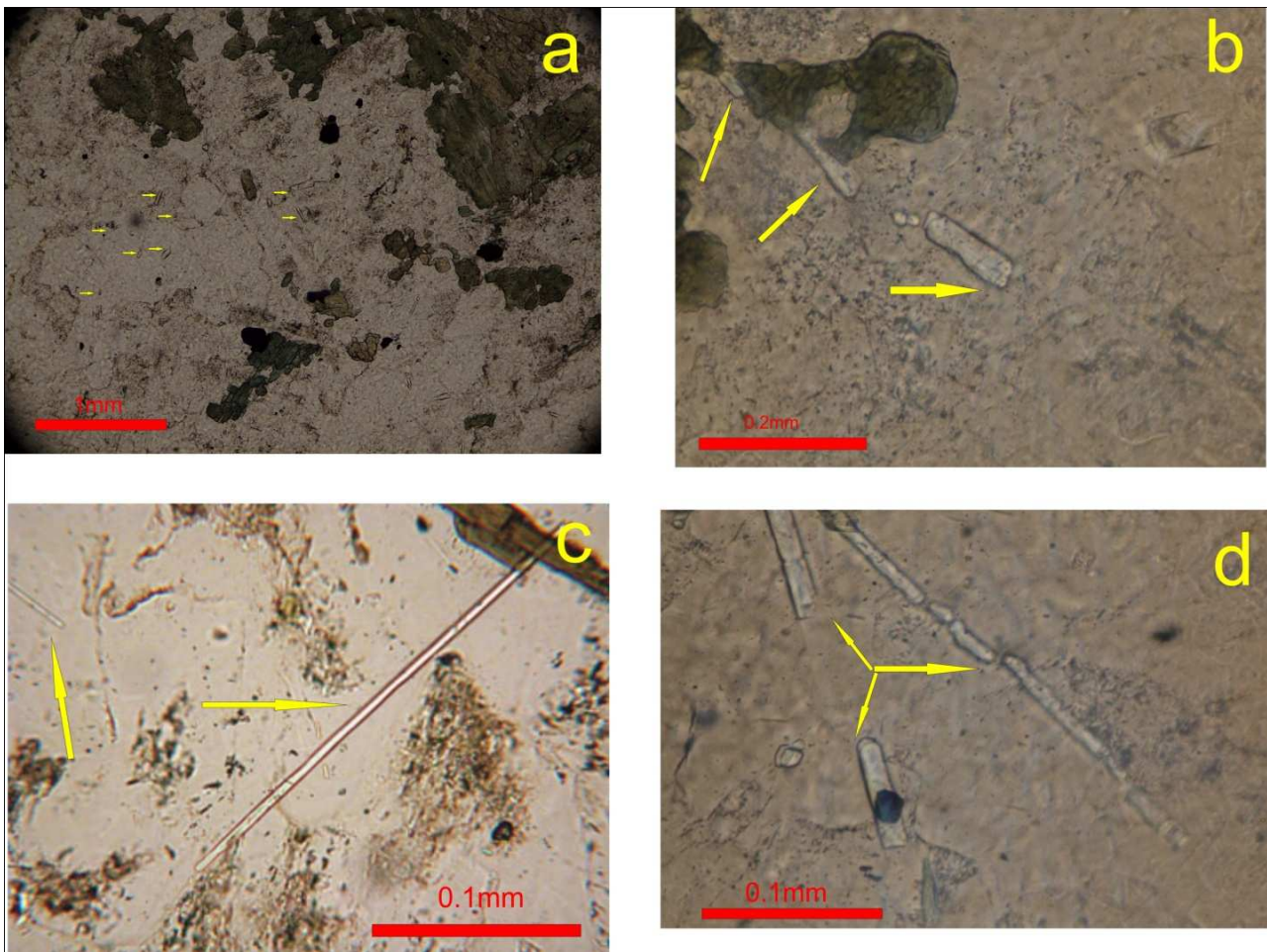
Fig. 4. Textural relations of different apatite grains in Zouzan granitoids. (a) Various apatite forms are distributed in granitoid groundmass. (b) Tabular and circular apatites; (c) acicular apatite in granodioritic sample; (d) elongated apatite needles in granitic sample. Yellow arrows show apatite grains. All figures are in PPL.

7. Conclusion

Electron micro probe analyses (EPMA) of apatite from different granitoid rocks indicate that many trace elements of apatite have concentration more than EPMA detection limit. Trace elements show different variations between various granitic types and could be effective tool to study granite petrogenesis and discriminate different type of them. Zouzan granitoids contain apatites with lower Fe, Mn, Na and HREE and higher LREE relative to typical S-type granites. Apatite composition is affected by magmatic evolution during Zouzan pluton petrogenesis. The concentration of Mn, Fe and Na in apatites increases during magmatic fractionation while Sr and REE falls. Different diagrams show that apatite chemistry is related to host rock and whole ASI could be defined as an indicator for discrimination of apatite variations. Strontium content of apatite is dependent on the host rock composition; and SrO concentration of apatites demonstrates nice correlations with other constituents which is in agreement with magmatic processes of Zouzan granitoids. The REE concentration of apatites from Zouzan granitoids have been impacted by contemporaneous crystallization of other minerals, especially accessory minerals. Amphibole crystallization could lead to HREE depletion in granodiorites and titanite fractionation could be responsible for LREE depletion in the felsic granitic samples.
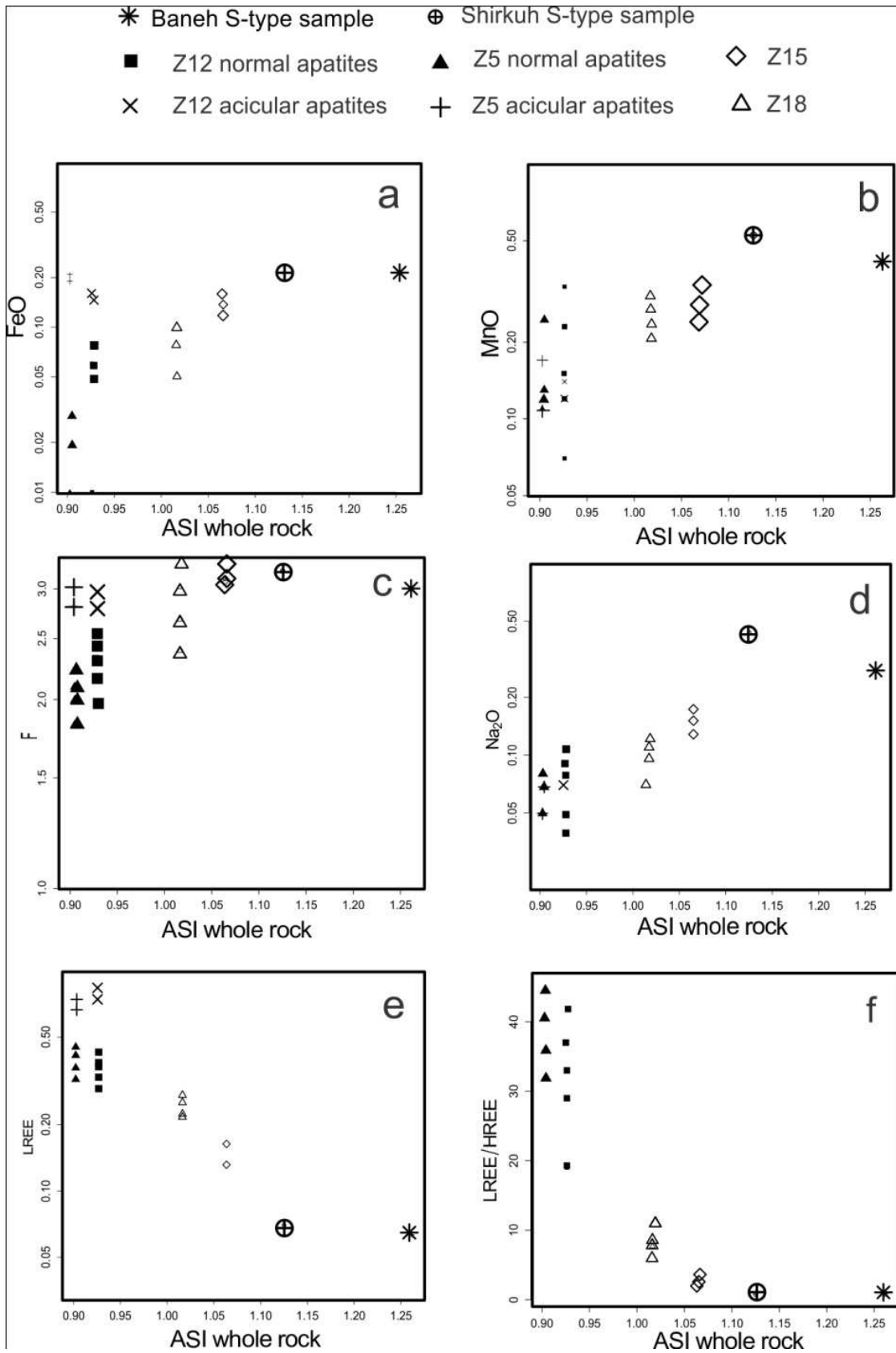
Fig. 5. Binary diagrams showing the relation of ASI host rock with trace elements of apatites.
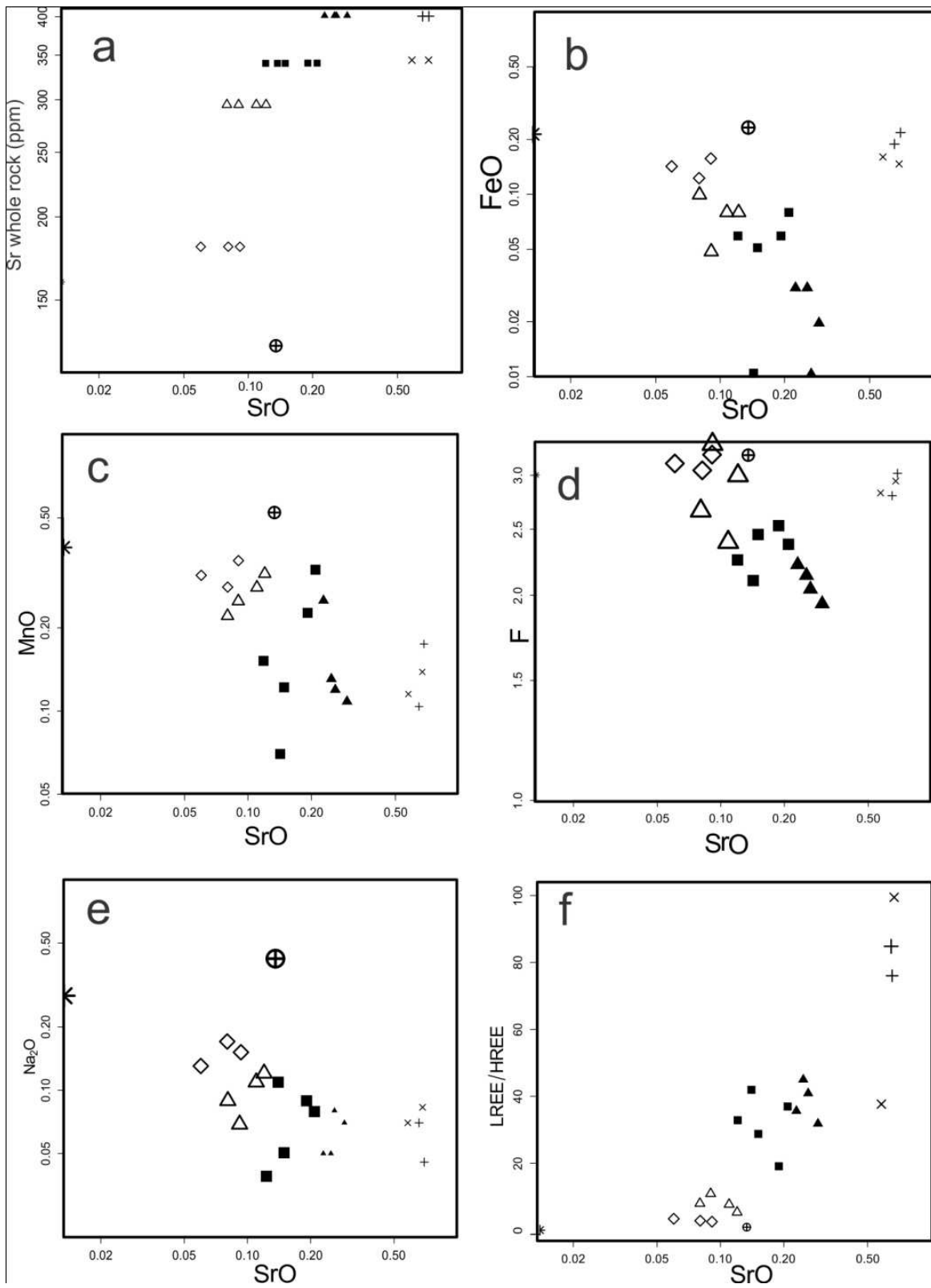
Fig.6. Host rock Sr and trace element variation of apatite as a function of SrO content of apatite. Symbols are similar to Fig. 5.

Acknowledgment

References

[1] Watson E. B.,1980, Apatite and phosphorus in mantle source regions: An experimental study of apatite/melt equilibria at pressures to 25 kbar: Earth and Planetary Science Letters, v. 51, p.322–335.

[2] Hoskin, P.W. O., Kinny, P. D.,Wyborn, D. & Chappell, B.W., 2000, Identifying accessory mineral saturation during differentiation in granitoids magmas: an integrated approach: Journal of Petrology, v.41, p.1365-1396.

[3] Treloar, P.J., Colley, H., 1996, Variations in F and Cl contents in apatites from magnetite–apatite ores in northern Chile, and their ore-genetic implications: Mineralogical Magazine, v.60, p.285–301.

[4] Belousova, E.A., Griffin, W.L., O'Reilly, S.Y., Fisher, N.I., 2002, Apatite as an indicator mineral for mineral exploration: trace-element compositions and their relationship to host rock type: Journal of Geochemical Exploration, v.76, p.45–69.

[5] Meurer, W.P., Natland, J.H., 2001, apatite compositions from oceanic cumulates with implications for the evolution of mid-ocean ridge magmatic systems: Journal of Volcanology and Geothermal Research, v.110, p.281-298.

[6] Boyce, J.W., Hervig, R.L., 2010, Apatite as a monitor of late-stage magmatic processes at Volca´n Irazu´ , Costa Rica: Contribution to Mineralogy and Petrology, v.157, p.135–145.

[7] Brassinnes, S., Balaganskaya, E., Demaiffe, D., 2005, Magmatic evolution of the differentiated ultramafic, alkaline and carbonatite intrusion of Vuoriyarvi (Kola Peninsula, Russia). A LA-ICP-MS study of apatite: Lithos, v.85, p.76-92.

[8] RØnsbo, J.G., 2009, Apatite in the Ilímaussaq alkaline complex: Occurrence, zonation and compositional variation: Lithos, v.106, p.71-82.

[9] Sha, L.K., Chappell, B.W., 1999, Apatite chemical composition, determined by electron microprobe and laser-ablation inductively coupled plasma mass spectrometry, as a probe into granite petrogenesis: Geochimica et Cosmochimica Acta, v.63, p.3861–3881.

[10] Broska, I., Williams, C.T., Uher, P., Konecny, P., Leichmann, J., 2004, The geochemistry of phosphorus in different granite suites of the Western Carpathians, Slovakia: the role of apatite and P-bearing feldspar: Chemical Geology, v.205, p.1-15.

[11] Hsieh, P.-S., Chen, C.-H., Yang, H.-J. & Lee, C.-Y., 2008, Petrogenesis of the Nanling Mountains granites from South China: constraints from systematic apatite geochemistry and whole-rock geochemical and Sr-Nd isotope compositions: Journal of Asian Earth Sciences, v.33, p.428-451.

[12] Chu, M.F., Wang, K.L., Griffin, W.L., Chung, S.L., Oreilly, S.Y., Pearson, N.J., Iizuka, Y., 2009, Apatite Composition: Tracing Petrogenetic Processes in Transhimalayan Granitoids: Journal of Petrology, v.50, p.1829-1855.

[13] Mazhari, S.A., Safari, M., 2012, High-K calc-alkaline plutonism in Zouzan, NE of Lut block, Eastern Iran: an evidence for arc related magmatism in Cenozoic: Journal of Geological Society of India, (accepted, in press).

[14] Nabavi, M.H., 1976, Intruduction to Geology of Iran: Geological Survey of Iran press (in Farsi).

[15] Takin M., 1972, Iranian geology and continental drift in the Middle East: Nature, v. 235, p.147–150.

[16] Davoudzadeh M, Schmidt K., 1984, A review of the Mesozoic paleogeography and paleotectonic evolution of Iran: Neues Jb Geol Paläont Mh, v.168, p.182–207.

[17] Tarkian, M., Lotfi, M., Baumann, A., 1983, Tectonic, magmatism and the formation of mineral deposits in the central Lut, east Iran, Ministry of mines and metals, GSI, geodynamic project (geotraverse) in Iran, No. 51, p.357-383.

[18] Westphal, M., Bazhenov, M.L., Lauer, J.P., Pechersky, D.M., Sibuet, J.C., 1986, Paleomagnetic implications on the evolution of the Tethys belt from the Atlantic ocean to the Pamirs since the Triassic: Tectonophysics, v. 123, p.37–82.

[19] Tirrul R, Bell LR, Grrifis RJ, Camp V.E.,1983, The Sistan suture zone of eastern Iran: Geological Society of America Bulletin, v.84, p.134–150.

[20] Mirnejad, H., Blourian, G.H., Kheirkhah, M., Akrami, A.M., Tutti, F., 2008, Garnet-bearing rhyolite from Deh-Salm area, Lut block, Eastern Iran: anatexis of deep crustal rocks: Mineralogy and Petrology, v.94, p.259-269.

[21] Karimpour, M.H., Stern, C.R., Farmer, L., Saadat, S., Malekzadeh, A., 2011, Review of age, Rb-Sr geochemistry and petrogenesis of Jurassic to Quaternary igneous rocks in Lut Block, Eastern Iran: Journal of Geopersia, v.1, p.19-36.

[22] Blourian, G.H., Safari, M., 2005, Geological map of Zouzan: Tehran, Geological Survey of Iran, scale 1:100000 (in Farsi).

[23] Mazhari, S.A., 2003, Petrological and geochemical study of igneous bodies of West Baneh (Kordistan): MSc thesis, Tarbiat Moallem University of Tehran, 158pp (in Farsi).

[24] Sheibi, M., Esmaeily, D., Nedelec, A., Bouchez, J.L., Kananian, A., 2010, Geochemistry and petrology of garnet-bearing S-type Shir-Kuh granite, southwest Yazd, Central Iran: Island Arc, v.19, p.292-312.

[25] Chappell, B. w., White, A.J.R., 1992, I- and S- type granite in Lachlan Fold Belt: Transactions of Royal Society of Edinburg Earth Science, v.83, p.1-26.

[26] Chappell, B. w., White, A.J.R., 2001, Two contrasting granite types: 25 years later: Australian Journal of Earth Science, v.48, p.489-499.

[27] Nash, W.P., 1984, Phosphate minerals in terrestrial igneous and metamorphic rocks. In: Nriagu, J.O., Moore, P.B. (Eds.): Phosphate Minerals, Springer-Verlag, Berlin, p. 442.

[28] Bea, F., 1996, Residence of REE, Y, Th and U in granites and crustal ptotoliths; implications for the chemistry of crustal melts: Journal of Petrology, v.37, p.521-552.